MECHANICAL PERFORMANCE OF A MANIPULATOR IN VIRTUAL REALITY SYSTEMS

Jose San Martin

Department of Computers Architecture, Universidad Rey Juan Carlos, Madrid, Spain

Gracian Trivino

Department of Photonic Technology, Universidad Politecnica, Madrid, Spain

Keywords: Virtual reality, Haptic interface, Manipulability, Mechanical Performance.

Abstract: Frequently, the human interface of a virtual reality system includes a 3D manipulator. In order to optimize the use of this device, the designer must take into account its mechanical characteristics. An obvious design criterion consists of maximizing the coincidence between the application 3D space and the physical volume where the manipulator provides its maximum performance. This paper explains in detail the analysis of manipulability for the PHANToM OMNi haptic device including the study of the manipulability distribution into its real workspace boundaries. As result of this study we will define a measure of the quality of the device placement inside the virtual reality system platform. We apply this measure for designing the mechanical configuration of a simulator for Minimally Invasive Arthroscopic Surgery.

1 INTRODUCTION

1.1 Object of Study

At the moment of evaluating the performance of a mechanical manipulator, one of the elements to consider is its capability for reaching and moving around the different points belonging to the workspace. Depending on the application requirements and on the device features it will allow the transmission of movement and force with major or minor difficulty up to the end of the kinematics chain. These characteristics are associated with the concept of manipulability that this work describes thoroughly in section 4.

We use the PHANToM OMNi of SensAble Technologies, that is a well known haptic device (SensAble Technologies, 2004), to describe and demonstrate the contributions of this work.

1.2 Defining Workspaces

We introduce three definitions relative to the device working area:

(a) Nominal Workspace (NW). This is the volume in which the manufacturer guarantees the specified force feedback and precision. For the OMNi device it is a rectangular prism of dimensions 160 W x 120 H x 70 D mm.

(b) Real Workspace (RW). This is the volume that we can reach with the End Effector. Note that RW includes a marginal zone where performance of the device can be unacceptable for some applications.

(c) Effective Workspace (EW). It is the volume of the application, so it is different in each system. For instance it is the working space used by a surgeon inside of a knee in a simulation of Minimally Invasive Surgery. In this paper we will show the relevancy of the shape and size of the EW for the aim of obtaining a good device performance.

1.3 PHANTOM OMNi Device

Figure 1 identifies the main mechanical components of the OMNi device: Element A (Head) turns around Y axis (yaw), defining angle θ_1. Element B (Crank) turns around X axis (pitch), defining angle θ_2. Element C (Connecting Rod) turns around X' relative axis (pitch), defining angle θ_3. Elements D

(Wrist), E (Fork) and F (Stylus) turn around orthogonal axes located at the End Effector and are the Gimbal angles.
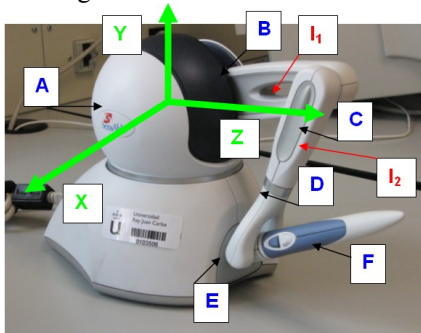

Figure 1: Different Components of the OMNi device. Coordinate System (CS) XYZ in the origin. Arms l_1=129mm and l_2=133 mm.

As far as we are interested in study the movement of the point where force feedback is applied, we will not consider the three gimbal elements (D, E and F).

Table 1: Relative values of θ_3 depending on θ_2 (value of the angles in degrees).

θ_2	$\theta_{3\ minimum}$	$\theta_{3\ maximum}$
0	-20	65
15	-15	90
30	-9	105
40	0	110
50	10	112
60	20	113
80	40	114
90	50	114
105	60	110

For this device, values of θ_1 range from -50º to 55º and values of θ_2 range from 0º to 105º. Note that there is kinematics cylindrical symmetry for θ_1 values. Due to the Omni mechanical design, range of θ_3 is not constant and depends on the value of θ_2 and on the angle inter-arms (l_1-l_2). Table 1 shows the correspondence between these angles.

2 KINEMATICS

References (Cavusoglu, Feygin and Tendick, 2002) and (Rodriguez and Basañez, 2005) describe a similar kinematics analysis of a former PHANToM haptic device version.

In this study the Coordinate System Origin (CSO) is the center of the element A.

2.1 Forward Kinematics

It is the expression of the End Effector position in Cartesian coordinates in function of the angles of the joints θ_i:

$$(x, y, z) = F(\theta_1, \theta_2, \theta_3)$$

From the geometrical relations between the elements in figure 2, adding sequentially the transformations T01, T02 and T03, we obtain the transformation matrix T04 from CSO to the End Effector position:

$$\begin{pmatrix} \cos(\theta_1) & -\sin(\theta_1)\sin(\theta_3) & \cos(\theta_3)\sin(\theta_1) & l_1\cos(\theta_2)\sin(\theta_1)+l_2\sin(\theta_1)\sin(\theta_3) \\ 0 & \cos(\theta_3) & \sin(\theta_3) & -l_2\cos(\theta_3)+l_1\sin(\theta_2) \\ -\sin(\theta_1) & -\cos(\theta_1)\sin(\theta_3) & \cos(\theta_1)\cos(\theta_3) & l_1\cos(\theta_1)\cos(\theta_2)+l_2\cos(\theta_1)\sin(\theta_3) \\ 0 & 0 & 0 & 1 \end{pmatrix}$$

Where the sub-matrix R04, is the system rotation matrix:

$$R04 = \begin{pmatrix} \cos(\theta_1) & -\sin(\theta_1)\sin(\theta_3) & \cos(\theta_3)\sin(\theta_1) \\ 0 & \cos(\theta_3) & \sin(\theta_3) \\ -\sin(\theta_1) & -\cos(\theta_1)\sin(\theta_3) & \cos(\theta_1)\cos(\theta_3) \end{pmatrix}$$

And the coordinates of the End Effector referred to CSO are the last column of T04.

$$x = (l_1\cos\theta_2 + l_2\sin\theta_3)\sin\theta_1$$
$$y = l_1\sin\theta_2 - l_2\cos\theta_3$$
$$z = (l_1\cos\theta_2 + l_2\sin\theta_3)\cos\theta_1$$

2.2 Inverse Kinematics

It consists of the expression for the angles θ_i of each joint in function of the End Effector position Cartesian coordinates:

$$(\theta_1, \theta_2, \theta_3) = I(x, y, z)$$

Almost directly and using the cosine theorem we obtain:

$$\theta_1 = -\arctan(\frac{x}{z}) \ ;$$
$$\theta_2 = \arctan(\frac{y}{H}) + \arccos(\frac{L^2 + l_1^2 - l_2^2}{2l_1L})$$
$$\theta_3 = \arctan(\frac{H - l_1\cos\theta_2}{l_1\sin\theta_2 - y})$$

3 JACOBIAN CALCULATION

Given a function F: $R^n \rightarrow R^m$ with m components y_1 to y_m each of them with n independent variables x_1 to x_n, the Jacobian consists of the matrix of partial derivatives of y_i respect of each one of the x_i.

$$J = \begin{pmatrix} \dfrac{\partial y_1}{\partial x_1} & \cdots & \dfrac{\partial y_1}{\partial x_n} \\ \dot{\partial y_m}{\partial x_1} & \cdots & \dfrac{\partial y_m}{\partial x_n} \end{pmatrix}$$

The upper half of the Jacobian represents the relation that exists between the linear velocities of the End Effector with the angular velocity of the joints:

$$V = Ju \cdot d\theta/dt$$

The lower half represents the relation between the angular velocity of the End Effector with the angular velocity of the joints:

$$\omega = J_l \cdot d\theta/dt$$

In the case of the OMNi, upper half of the J has the dimensions (3xn) where n is the number of degrees of freedom. For this device the Jacobian is:

$$J = \begin{pmatrix} l_1\cos(\theta_2) + l_2\sin(\theta_3) & 0 & 0 \\ 0 & l_1\cos(\theta_2 - \theta_3) & 0 \\ 0 & -l_1\sin(\theta_2 - \theta_3) & l_2 \\ 0 & 0 & -1 \\ \cos(\theta_3) & 0 & 0 \\ \sin(\theta_3) & 0 & 0 \end{pmatrix}$$

4 MANIPULABILITY

Manipulability is the skill in transmitting movement and applying forces in arbitrary directions (Park and Kim, 1998). We can also say that the manipulability of a device indicates its ability to move freely in all the directions in the workspace (Murray, Li and Sastry, 1994). Another definition is that manipulability is the efficiency with which a manipulator transmits force and velocity to its End Effector (Staffetti, Bruyninckx and De Schutter, 2002).

4.1 Calculation of Manipulability Map

The manipulability of a device was conceptually defined by (Salisbury and Craig, 1982) and the first formulation that allowed a mathematical simple quantification was brought up by (Yoshikawa, 1985).

A widely used algebraic definition of manipulability is the one by (Yoshikawa, 1990).

$$\mu = \sqrt{\det(Ju * Ju')},$$

Where Ju is the upper part of the Jacobian and Ju' is its transposed one. Others authors propose different formulations for the Manipulability. For example (Cavusoglu, Feygin and Tendick, 2002) (Tavakoli, Patel and Moallem, 2004) make use of:

$$\mu = \sigma_{min}(J_u)/\sigma_{max}(J_u) \qquad (1)$$

Where σ_{min} and σ_{max} are the minimum and the maximum of the singular values of J_u.

4.2 Map of Manipulability

Figure 2 shows the map of curves of iso-manipulability in the plane X=0 ($\theta_1 = 0$) calculated by (1). Because the Jacobian does not depend on θ_1, the manipulability is equal for any plane defined by a value of θ_1.
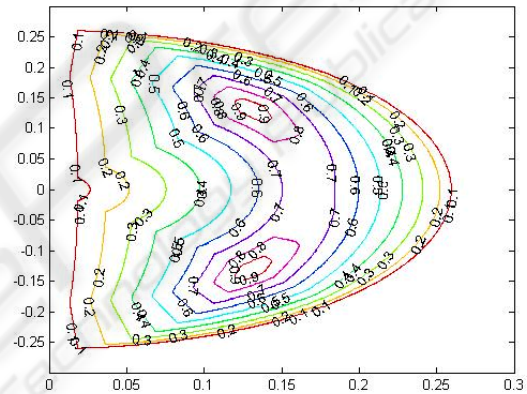

Figure 2: Iso-manipulability curves map for plane X=0. Axis values in meters. Curves contain values of µ.

4.3 Real Workspace

According to the θ_1, θ_2 and θ_3 ranges in table 1 we can describe the maximum area that End Effector can reach in the plane YZ. The real workspace-RW is defined by this curve. This evolving curve is projected on the map of manipulability and so we can extract the portion of the map that the End Effector can really reach (fig. 3).
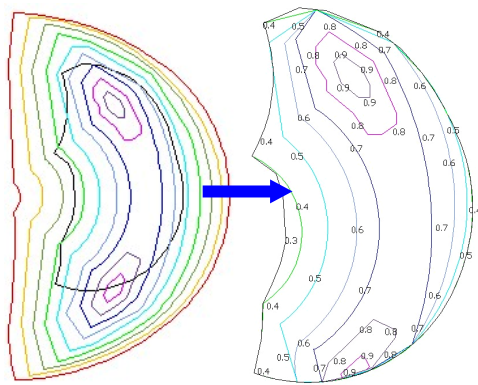
237

Figure 3: Projection of the real workspace on the manipulability map and Subspace of manipulability defined for the real workspace.

Note that, in the Omni device, the best values of manipulability are included in the real working area.

5 3D MAP OF MANIPULABILITY

Integrating the 2D surfaces of iso-manipulability we can generate volumes containing points with equal value of μ. Figure 4 shows the 3D Map of Manipulability associated to the PHANToM OMNi device. It will be useful to the designer of a new virtual reality system to consider this volume as a virtual part of the OMNi.
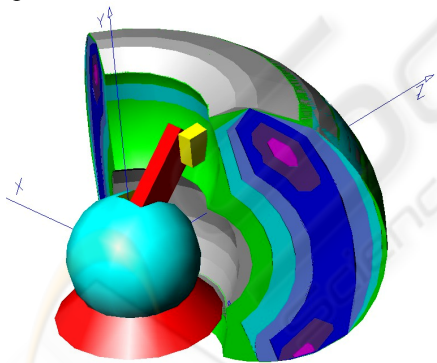

Figure 4: Scheme of the 3D Map of Manipulability for the OMNi.

6 VOLUMETRIC AVERAGE MANIPULABILITY

This section concerns with the study of how to situate the OMNi in the system mechanical platform to obtain its maximum performance.

The EW is a 3D volume that must be situated inside the 3D map of Manipulability. The intersection from both solids determines different values of μ in EW indicated by different sub volumes v_i (different colors in figure 4). The total volume V_T is:

$$V_T = \sum_i^n v_i = v_1 + v_2 + ... + v_n$$

We define Volumetric Average Manipulability as:

$$\mu_v = \frac{(\mu_1 \cdot v_1 + \mu_2 \cdot v_2 + \mu_3 \cdot v_3 + ... \mu_n \cdot v_n)}{V_T} \quad (2)$$

Where μ_i is the Manipulability in each v_i.

This measure is useful to do a quantitative comparison between different possible mechanical configurations of a system using manipulators.

7 THEORETICAL EXAMPLES

We have designed four tests, each one with two options for placing the Effective Workspace, in order to verify the usability of the Volumetric Average Manipulability μ_v.

Test A. EW is a cube of L=100mm:

Case A1. We place the center of gravity (CG) at 150 mm from the origin along the axis Z. After calculation, formula (2) produces: μ_v =0.5411.

Case A2. We place it in the neighborhood of the optimal manipulability values zone, CG at position XYZ (-10, 94, 151) mm. After calculation it produces: μ_v = 0.7103 sensitively higher.

Figure 5 shows the intersections of the EW with the solid of manipulability. Cases A1 and A2.
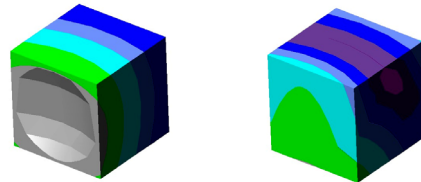

Figure 5: Intersection of the workspaces with the solid of manipulability.Test A.

Test B. EW is a rectangular squared-base prism of side L=100mm and height H=200mm:

Case B1. CG of the prism at (-10, 14, 151). The Manipulability obtained is μ_v =0.6422 (fig. 6).

Case B2. We situate it, lying down on a plane parallel to the XZ, fitting in the ideal zone of manipulability. First we translate GC of the prism at (5, 92, 161) and a turning of 45 º with regard to an axis parallel to the Z axis that crosses the CG. The

value obtained is μ_v=0.7353 (fig. 6). Note that this high value has been obtained by inclining the OMNi.
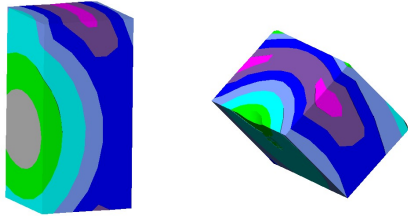

Figure 6: Intersection of the EW with the solid of manipulability. Test B.

Test C. EW is an L-shaped solid of side L=50mm + rectangular prism of square base of side L=50mm and height H=100mm:

Here, not only it is need to align the EW with the optimal zone of the manipulability map, but also to modify the orientation. For the case C1 it has been obtained a value of μ_v =0.7730 (fig. 7). In the second case C2 by means of two turning, we get a value of μ_v=0.8336 (fig. 11).
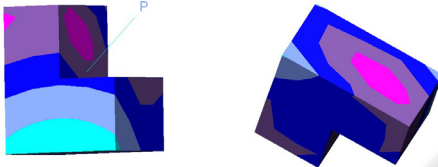

Figure 7: Intersection of the EW with the solid of manipulability. Test C.

Test D. EW is a solid of revolution axis Y (D: 100 mm): cylinder (H: 90 mm) with a cone (H: 50mm) in each of the bases and a hollow in its interior.

Case D1. Turn of -90º around axis Z. We move the CG from CSO at position XYZ (21, 107, 148). After calculation it produces: μ_v =0.7618 (fig. 8).

Case D2. Turn of -90º around axis Z. We move the CG from CSO at position XYZ (-14, 114, 163) avoiding the hollow of the solid. After calculation it produces: μ_v =0.7829 (fig. 8).
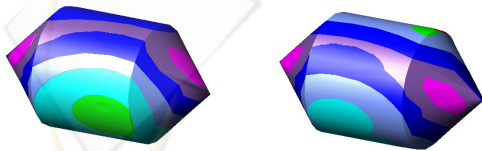

Figure 8: Intersection of the EW with the solid of manipulability. Test D.

This Test D simulates a more complex and not homogeneous EW, similar to a cavity in a virtual surgical simulation, being the hollow an unreachable space, for example a bone, where we are not interested in optimizing μ.

8 DESIGN OF AN APPLICATION

This section describes a real application of the ideas developed above. It consists of the positioning of the OMNi device when used as a component of a simulator for training in Minimally Invasive Arthroscopic Surgery (Bayona, Garcia, Mendoza and Fernandez, 2006), (GMV, 2006). This study is centered in a virtual model of the human left shoulder.

Figure 9-1 shows an anatomical model of this joint where the subacromial capsule has been suppressed. In this case the EW has two spaces quite differenced that we name EW-glenohumeral and EW-subacromial.
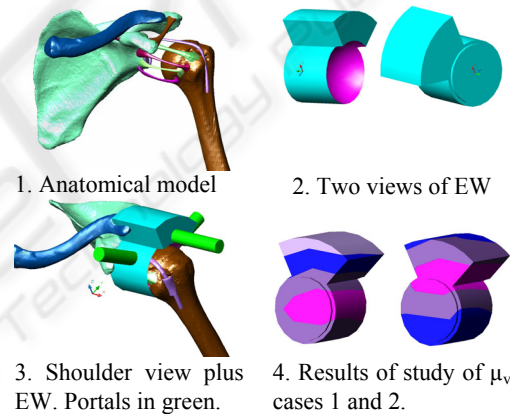

1. Anatomical model

2. Two views of EW

3. Shoulder view plus EW. Portals in green.

4. Results of study of μ_v cases 1 and 2.

Figure 9: Study of μ_v in a real implementation.

EW-glenohumeral is the domain of surgeries such as acromioplasty and it has been modeled using two cylinders and a spherical hollow. EW-subacromial is the domain of surgeries such as arthroscopic labrum fixation and it has been modeled using a pipe sector. Nevertheless there are operations, as the diagnostic arthroscopy, which cover both spaces (Giacomo and Constantini, 2004). Figure 9-2 shows two views of the whole EW.

Figure 9-3 shows this EW in its placement into the anatomical model. Note that portals for surgical instrumentation access (green colored in the figure) are not included in the μ_v study because that space has not meaningful value. Also here, two cases have been considered (fig. 9-4):

Case 1. EW situated matching the CG of EW-glenohumeral with the maximum manipulability zone; position XYZ (85, 118, 148). The aim of this

approach is obtaining optimal manipulability values in EW-glenohumeral. After calculation it produces: μ_v=0.8073 in the whole of EW. Analyzing them separately, we obtain μ_v=0.8873 for EW-glenohumeral and μ_v=0.7194 for EW-subacromial.

Case 2. CG of EW situated at maximum manipulability zone, position XYZ (85, 118, 148). The criterion is to obtain maximum average manipulability values for all the EW. After calculation it produces: μ_v=0.8506 in the whole of EW. Analyzing them separately, we obtain μ_v=0.8291 for EW-glenohumeral and μ_v=0.8749 for EW-subacromial.

9 CONCLUSIONS

A complete study about different workspaces to distinguish in the environment of a haptic device has been analyzed.

The need of establishing a criteria for helping the mechanical design of a simulator of Minimally Invasive Arthroscopic Surgery has lead us to contribute in this field by creating a measure that we have called Volumetric Average Manipulability (μ_v). A set of different configurations can be valued in order to choose the best option. This new concept will be able to help in the optimal design of a system involving some haptic device.

The use of this measure has been demonstrated in several cases of theoretical Effective Workspaces. A study on the real case of a virtual human shoulder joint involving the PHANToM OMNI haptic device has been presented.

ACKNOWLEDGEMENTS

REFERENCES

Bayona S., Garcia M., Mendoza C., Fernandez, J.M., Shoulder Arthroscopy Training System with Force Feedback, pp. 71-76, *International Conference on Medical Information Visualisation-BioMedical Visualisation (MedVis'06),* 2006.

Cavusoglu, M. C., & Feygin, D. and Tendick F. A Critical Study of the Mechanical and Electrical Properties of the PHANToM Haptic Interface and Improvements for High Performance Control. *Teleoperators and Virtual Environments,* 11(6):555--568, 2002.

Di Giacomo, G. Costantini, A. Arthroscopic shoulder surgery anatomy: Basic to advanced portal placement. *Operative Techniques in Sports Medicine,* Volume 12, Issue 2, Pages 64-74 G, 2004.

GMV, Universidad Rey Juan Carlos, Universidad Politecnica de Madrid, Hospital Severo Ochoa de Leganes, Virtual Reality Arthroscopy Trainer. Technological Innovation for improving minimally invasive surgery skills, 2006. http://www.insightmist.com/index_en.htm

Murray, R. M., Li, Z., & Sastry, S. S. (1994). A mathematical introduction to robotic manipulation. CRC Press, Inc. Boca Raton, FL.

Park, F., Kim, J., Manipulability of Closed Kinematic Chains, *in J. Mech. Des.,* Vol. 120, Dec. 1998.

Rodriguez, A., Basañez, L. (2005). Modelo cinematico de la interface háptica PHANToM Premium 1.5/6DOF. (Tech. Rep.). Universidad Politecnica de Cataluña. Instituto de Organización y Control de Sistemas Industriales.

Salisbury, J.K., and Craig, J. J., Articulated hands: force control and kinematic issues, *Int. J. Robotics Research, Vol. 1* no. 1, 1982, pp. 4-17.

SensAble Technologies. PHANToM OMNi User's Guide. November 2004.

Staffetti, E., Bruyninckx, H. & De Schutter, J. 2002. On the Invariance of Manipulability Indices. J. Lenarcic and F. Thomas (eds.), Advances in Robot Kinematics, Kluwer Academic Publishers: 57-66.

Tavakoli, M., Patel, R.V. and Moallem M. (2004) Design Issues in a Haptics-Based Master-Slave System for Minimally Invasive Surgery. *In proceedings of the 2004 IEEE International Conference on Robotics and Automation (ICRA '04),* pp. 371-376, New Orleans, LA.

Yoshikawa, T.; Manipulability and redundancy control of robotic mechanisms, *Robotics and Automation. Proceedings of IEEE International Conference on,* Volume 2, Mar 1985 Page(s):1004 – 1009.

Yoshikawa, T.; Foundations of Robotics: Analysis and Control. Cambridge, MA: MIT Press, 1990.